



HAL
open science

Dramatic effect of the nature of R on the intrinsic acidity and basicity of potential astrochemical R-C COH and R-C CSH compounds

Otilia Mó, Ibon Alkorta, Jean-Claude Guillemin, Manuel Yáñez

► **To cite this version:**

Otilia Mó, Ibon Alkorta, Jean-Claude Guillemin, Manuel Yáñez. Dramatic effect of the nature of R on the intrinsic acidity and basicity of potential astrochemical R-C COH and R-C CSH compounds. *Theoretical Chemistry Accounts: Theory, Computation, and Modeling*, 2023, 142 (3), pp.28. 10.1007/s00214-023-02967-0 . hal-04057661

HAL Id: hal-04057661

<https://hal.science/hal-04057661>

Submitted on 4 Apr 2023

HAL is a multi-disciplinary open access archive for the deposit and dissemination of scientific research documents, whether they are published or not. The documents may come from teaching and research institutions in France or abroad, or from public or private research centers.

L'archive ouverte pluridisciplinaire **HAL**, est destinée au dépôt et à la diffusion de documents scientifiques de niveau recherche, publiés ou non, émanant des établissements d'enseignement et de recherche français ou étrangers, des laboratoires publics ou privés.



Distributed under a Creative Commons Attribution 4.0 International License



Dramatic effect of the nature of R on the intrinsic acidity and basicity of potential astrochemical R–C≡COH and R–C≡CSH compounds

Otilia M^ó¹ · Ibon Alkorta² · Jean-Claude Guillemin³ · Manuel Yáñez¹

Received: 11 January 2023 / Accepted: 14 February 2023 / Published online: 3 March 2023
© The Author(s) 2023

Abstract

The effect of changing the nature of the R substituent from the first row (H, Li, BeH, BH₂, CH₃, NH₂, OH and F) to second row (Na, MgH, AlH₂, SiH₃, PH₂, SH and Cl) on the intrinsic acidity and basicity of R–C≡COH and R–C≡CSH compounds was investigated through the use of G4 high-level *ab initio* calculation. The variation of the acidity and basicity of the R–C≡CSH derivatives as a function of R is practically parallel to that found for the corresponding R–C≡COH analogs; though the basicities of the former are 9–14% higher than those of the latter, the acidity gap being very small (~2%). When this analysis is extended to the derivatives in which the triple CC bond is replaced by a double or single bond, it is found that the acidity gap increases systematically as the CC bond goes from triple to single; whereas, as expected for the basicity, the trend is the opposite. Quite surprisingly, however, the variation of the basicity of R–C≡CX (X = OH, SH) compounds with the nature of the first-row substituents, R, is remarkably different from that produced by the second-row analogs. The same is observed as far as intrinsic acidities are concerned. These dissimilarities reflect the rather different changes in the strength of the CC and the CX (X = OH, SH) bonds when a first-row substituent is replaced by the second-row analog, as reflected in the atoms in molecules (AIM), natural bond orbital (NBO) and the electron localization function (ELF) analyses of the corresponding species.

Keywords Ynols (R–C≡COH) · Ynethiols (R–C≡CSH) · Intrinsic acidity · Intrinsic basicity · G4 calculations

1 Introduction

Our information on the structure, stability and reactivity of small chemical compounds of astrochemical relevance is rather scarce. Many of the compounds detected in the interstellar medium are hard to be synthesized in the laboratory, and therefore, the information we have on their structure,

properties and reactivity is fragmentary, and much of it comes from theoretical approaches. Indeed, mainly along the last decade, a lot of information on the reactivity of many potential astrochemical compounds came from high-level *ab initio* calculations [1–8]. In a similar way, it was possible to determine the structure of new or potential astrochemical compounds [9–12] or predict their existence and/or their spectroscopic properties [12–26], or to explore their behavior in water or ice [27–29]. A fairly complete set of data on different astrochemical compounds have been compiled 2 years ago [30]. Still, as mentioned above, it is often extremely difficult to synthesize and analyze in the laboratory some specific astrochemical systems. A good example of compounds difficult to characterize experimentally is (Z)-1,2-ethenediol, the enol form of glycolaldehyde, which was detected for the first time in the interstellar medium very recently [31]. Quite unexpected, though the enthalpy of the formation of this enol was reported more than 30 years ago [32], it is rather unstable because of the larger stability of corresponding oxo forms [33]. The detection of (Z)-1,2-ethenediol in the interstellar medium (an isomer of the

✉ Ibon Alkorta
ibon@iqm.csic.es

✉ Manuel Yáñez
manuel.yanez@uam.es

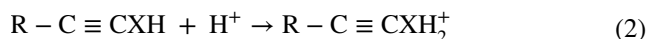
¹ Departamento de Química, Modulo 13, Facultad de Ciencias, and Institute for Advanced Research in Chemical Sciences (IAdChem), Universidad Autónoma de Madrid, Campus de Excelencia UAM-CSIC, Cantoblanco, 28049 Madrid, Spain

² Instituto de Química Médica, IQM-CSIC, Juan de la Cierva, 3, 28006 Madrid, Spain

³ Univ Rennes, Ecole Nationale Supérieure de Chimie de Rennes, CNRS, ISCR- UMR 6226, F-35000 Rennes, France

ubiquitous glycolaldehyde) suggests the possible existence of the analogous ethyne-1,2-diol ($\text{HOC}\equiv\text{COH}$) derivative, in which the $\text{C}=\text{C}$ double bond was replaced by a CC triple bond, but which was never synthesized. This situation is apparently the same when the OH groups are replaced by any other groups like in ethyne-1,2-diamine ($\text{H}_2\text{NC}\equiv\text{CNH}_2$) for which an isomer has been detected, the aminoacetonitrile [34]. This prompted us to consider the importance of having precise information on the properties of this type of compounds, and how these properties can be modulated by changing the nature of the substituents that can be attached to the carbon atoms. To carry out such an assessment, we decided to systematically investigate, through the use of reliable molecular orbital calculations, the gas-phase basicity and acidity of $\text{R}-\text{C}\equiv\text{COH}$ compounds, when the R substituent is not only a hydroxyl group, but also any possible group from the first and second row of the periodic table (Li , BeH , BH_2 , CH_3 , NH_2 , OH , F , Na , MgH , AlH_2 , SiH_3 , PH_2 , SH and Cl). For the sake of completeness, taking into account that the sulfur-containing analogs are also of astrochemical relevance, we have also included in our theoretical survey the corresponding $\text{R}-\text{C}\equiv\text{CSH}$ series.

Acidities and basicities are calculated as the enthalpy or the free energy of reactions (1) and (2), respectively, at a temperature of 298.150 Kelvin and a pressure of 1.0 Atm.



where $\text{X}=\text{O}$, S .

Since as indicated in reaction (1), the acidity is the energy required to deprotonate the neutral compound; the larger the value of the enthalpy or the free energy of reaction (1), the smaller the acidity. The basicity is usually given as the negative of enthalpy or free energy of reaction (2) to use positive values. In our work, we will use enthalpies instead of free energies. However, our conclusions will not change; since, as shown in Figure S1 of the Supporting Information, for both acidities and basicities, the correlation between enthalpies and free energies is very good with excellent linear correlations between both magnitudes.

2 Computational details

To accurately describe the intrinsic reactivity patterns of the compounds under investigation, in particular their intrinsic basicities and acidities, it is unavoidable to use an accurate enough theoretical model, such as the Gaussian-4 (G4) theory [35]. The G4 method is actually a composite high-level *ab initio* formalism, based

on a wise combination of well-defined MP2, MP4 and CCSD(T) molecular orbital calculations with the aim of having an accurate description of dispersion interactions. The result is that G4 provides energetic outcomes for different thermodynamic properties of a large set of chemical compounds with an average absolute deviation of 3.47 kJ mol^{-1} [35].

In the G4 procedure, the final energies are obtained by combining contributions obtained through the use of Møller–Plesset perturbation theory up to the fourth order and CCSD(T) coupled cluster theory, with the final goal of accurately account for the electron correlation effects. To these MPn and CCSD(T) energy contributions, an estimation of the Hartree–Fock energy limit (HF_{limit}) together with two high-level empirical corrections is added, in order to ensure that the final energies are accurate up to a CCSD(T,full)/G3LargeXP + HF_{limit} level. These *ab initio* calculations are carried out on previously B3LYP/6-31G(2df,p) optimized geometries. The corresponding thermal corrections are also obtained at this DFT level of theory [35]. Although very few experimental measurements on the acidities of these kind of systems are available, we have calculated the gas-phase acidities of HCCH, EtOH and EtSH whose experimental gas-phase acidities and basicities are known [36–38], in order to check the reliability of our procedure. As shown in Table S1 of the Supporting Information, though the error of some experimental outcomes is large, the agreement between both sets, experimental and theoretical values is excellent.

In order to rationalize the bonding characteristics of the compounds under scrutiny, we have used three complementary procedures, namely, the atoms in molecules (AIM) theory [39], the natural bond orbital (NBO) method [40] and the electron localization function (ELF) formalism [41]. This AIM method is based on a topological analysis of the molecular electron density, $\rho(\mathbf{r})$, with the aim of locating its critical points, because the maxima of $\rho(\mathbf{r})$ are associated with the nuclei, whereas the first-order saddle points, usually named bond critical points (BCPs), located between two maxima indicate the existence of a bonding interaction, so that its electron density provides useful information on the strength and nature of the bond to which the BCP is associated. This procedure also provides useful structural information through the molecular graph of the system formed by the lines, generally named bond paths, connecting neighbor maxima and containing a BCP. All these calculations have been carried out by using the AIMAll (Version 11.12.19) code [42].

A useful complementary view can be reached through the use of localized hybrids and lone pairs obtained as local block eigenvectors of the one-particle density, in the framework of the natural bond orbital (NBO) method [40]. The characteristics of these hybrid orbitals and their weight

provide a rather realistic view of the bonding patterns stabilizing the system. On top of that, a second-order perturbation formalism, within this framework, permits to evaluate the interaction energies between occupied and empty orbitals contributing to the stability of the molecule.

The ELF approach analyzes the probability of finding, for a given chemical system, an electron in the same position as a reference electron with the same spin. This leads to the definition and classification of the areas in which the electrons of the system are distributed in monosynaptic and disynaptic (or polysynaptic) basins. The monosynaptic basins are associated with a single nucleus and correspond to core electrons and/or electron lone pairs. Conversely, the disynaptic (or polysynaptic) basins correspond to the two-center or more than two-center bonding regions.

3 Results and discussion

The optimized structures for the neutral, protonated and deprotonated forms of compounds included in this survey are provided in Table S2 of the Supporting Information. In Table 1, their G4-calculated gas-phase acidities and basicities are given.

Table 1 G4-calculated gas-phase acidities ($\Delta H_{\text{gas,acid}}$) and basicities ($\Delta H_{\text{gas,bas}}$) (all values in $\text{kJ}\cdot\text{mol}^{-1}$) for $\text{RC}\equiv\text{CX}$ derivatives ($\text{R}=\text{Li}$, BeH , BH_2 , CH_3 , NH_2 , OH , F , Na , MgH , AlH_2 , SiH_3 , PH_2 , SH , Cl ; $\text{X}=\text{OH}$, SH)

Compound	Gas-phase acidity ($\Delta H_{\text{gas,acid}}$)		Gas-phase basicity ($\Delta H_{\text{gas,bas}}$)	
	X=OH	X=SH	X=OH	X=SH
HCCX	1391.1 ^a	1386.5 ^b	622.9	705.6
LiCCX	1478.0	1473.6	762.6	837.9
BeHCCX	1322.4	1340.7	625.5	710
BH ₂ CCX	1315.3	1333.7	611.1	692.5
CH ₃ CCX	1420.5	1409.9	660.3	741
NH ₂ CCX	1436.3	1429.4	705.4	768.5
HOCCX	1422.6	1419.6	665.6	744.9
FCCX	1374.9	1390.8	623.3	708.3
NaCCX	1499.5	1479.8	794.3	867.5
MgHCCX	1373.9	1383.9	674.8	755.3
AlH ₂ CCX	1319.6	1340.7	638.7	722
SiH ₃ CCX	1328.1	1344.2	632.7	718.2
PH ₂ CCX	1349.8	1361.5	639.4	724.8
HSCCX	1367.1	1376.1	648.1	727.7
ClCCX	1361.3	1372.9	627.9	716

^aThis value is in good agreement with the MP4/6–311 + G** estimate of ref. [42] ($1390 \text{ kJ}\cdot\text{mol}^{-1}$) and with the G2-value reported in ref. [43] ($1391 \text{ kJ}\cdot\text{mol}^{-1}$)

^bThis value is in good agreement with the G2 estimate of ref. [43] ($1384 \text{ kJ}\cdot\text{mol}^{-1}$)

The first conspicuous fact, as illustrated in Fig. 1, is that the acidities and basicities of the OH and SH derivatives followed rather similar trends, as the variation of these two magnitudes with the nature of the R substituent yield curves, for both sets of derivatives, which are practically parallel. It can be also observed that the acidities do not only follow similar trends for both sets of compounds, but they are very close in such a way that the acidities for the OH derivatives differ from those of the SH counterparts by less than 2%. Also, for some first-row substituents ($\text{R}=\text{BeH}$, BH_2 , F), the SH derivatives are slightly less acidic than the OH ones, whereas for the second-row substituents, with the only exception of $\text{R}=\text{Na}$, the thio derivatives are systematically slightly more acidic than the oxy ones. For the basicities, however, the SH derivatives are found to be 9–14% more basic than the OH-containing analogs.

The first accurate acidity of $\text{HC}\equiv\text{COH}$ calculated at MP4/6–311 + G** level was reported back in 1989 by Radom et al. [43]. This value, $1390 \text{ kJ}\cdot\text{mol}^{-1}$, is in very nice agreement with an G2 estimation published in 2005 [44] and with the G4-value reported here (see Table 2), showing that ethynol should be slightly more acidic in the gas phase than HCl, whose reported experimental acidity ($1394.9 \text{ kJ}\cdot\text{mol}^{-1}$) is $4 \text{ kJ}\cdot\text{mol}^{-1}$ smaller [45]. The high gas-phase acidity predicted for ethynol is also coherent with the high acidity in aqueous solution measured for 2-phenylethynol, $\text{PhC}\equiv\text{COH}$, for which a $\text{pK}_a \leq 2.8$ was measured which is 7 pK_a units more acidic than its enol analog, $\text{PhCH}=\text{CHOH}$ [46]. Our G4 calculations also show that ethynethiol, $\text{HC}\equiv\text{CSH}$, is even more acidic than ethynol in very good agreement with the G2-values reported before [44]. Unfortunately, however, the experimental information on the gas-phase acidity and basicity of the $\text{C}\equiv\text{C}$ unsaturated compounds included in this study is totally inexistent, and only for the two saturated analogs, $\text{CH}_3\text{-CH}_2\text{X}$ ($\text{X}=\text{OH}$, SH), both properties are known [36], whereas for the $\text{CH}_2=\text{CHX}$ ($\text{X}=\text{OH}$, SH) compounds, only the experimental gas-phase acidity has been reported [44]. The surprising finding, however, is that when looking at the experimental acidities and basicities of the $\text{CH}_3\text{-CH}_2\text{X}$ ($\text{X}=\text{OH}$, SH) derivatives, it is observed that the gap between their acidities ($98 \text{ kJ}\cdot\text{mol}^{-1}$) is almost one order of magnitude larger than the gap between their basicities, whereas our theoretical results for the analogs with a CC triple bond show a completely opposite behavior, an acidity gap of only $4.6 \text{ kJ}\cdot\text{mol}^{-1}$ vs. basicity gap of $82.7 \text{ kJ}\cdot\text{mol}^{-1}$. This apparent contradiction moved us to investigate whether there is a significant effect of the unsaturation of the alkyl chain on these intrinsic properties. For this purpose, we have evaluated the gas-phase acidities and basicities of the three couples $\text{CH}_3\text{-CH}_2\text{X}$, $\text{H}_2\text{C}=\text{CHX}$ and $\text{HC}\equiv\text{CX}$ ($\text{X}=\text{OH}$, SH). The results obtained are summarized in Table 2.

It can be seen that the acidity and basicity gaps for the ethanol and ethanethiol are in very good agreement with

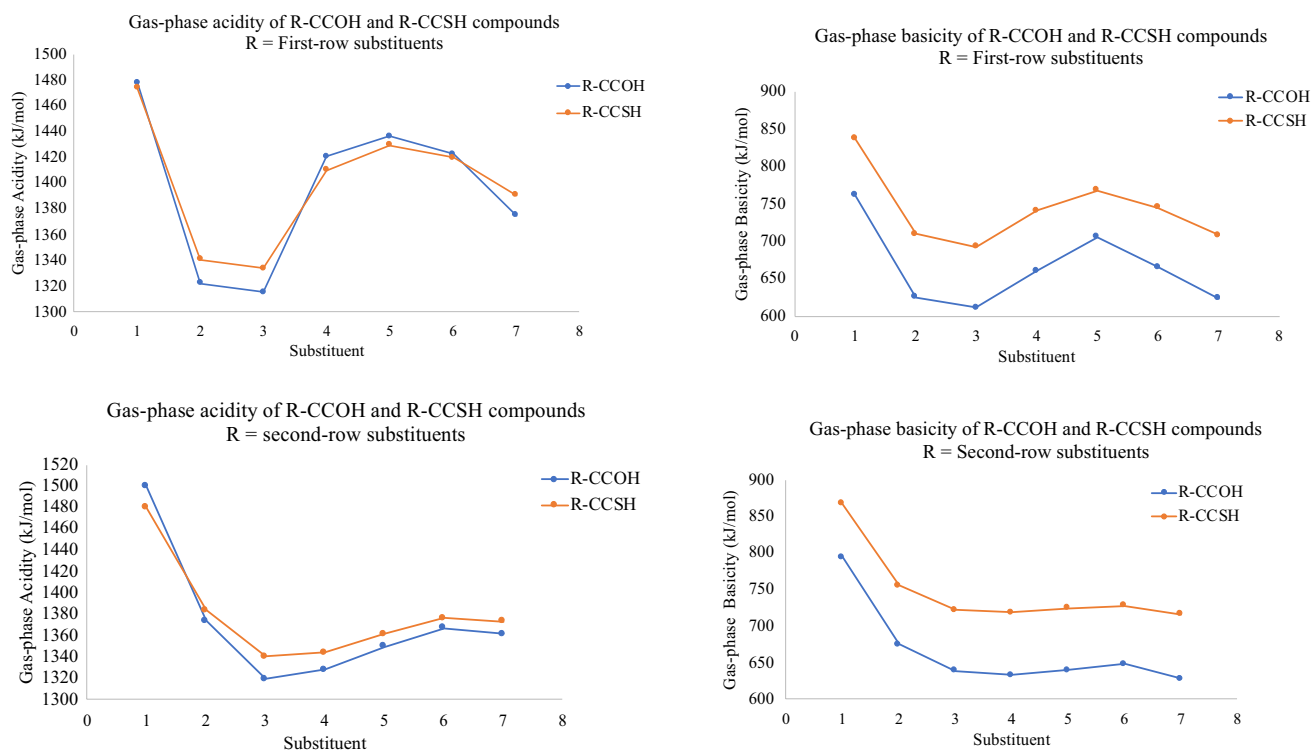


Fig. 1 Evolution of the gas-phase acidities and basicities for $RC\equiv COH$ and $RC\equiv CSH$ derivatives. R (first-row substituents) 1 = Li, 2 = BeH, 3 = BH_2 , 4 = CH_3 , 5 = NH_2 , 6 = OH and 7 = F. R (second-row substituents) 1 = Na, 2 = MgH, 3 = AlH_2 , 4 = SiH_3 , 5 = PH_2 , 6 = SH and 7 = Cl

Table 2 G4-calculated gas-phase acidity and basicity for CH_3-CH_2X , $H_2C=CHX$ and $HC\equiv CX$ ($X=OH, SH$) derivatives

Compound	Acidity ($\Delta H_{gas,acid}$)	Basicity ($\Delta H_{gas,bas}$)	$\Delta_{acidity}$	$\Delta_{basicity}$
CH_3-CH_2OH	1587.1 ^a	777.6 ^b	99.8	15.1
CH_3-CH_2SH	1487.4 ^a	792.7 ^b		
$H_2C=CHOH$	1489.8	725.0	45.5	35.2
$H_2C=CHSH$	1444.3	760.2		
$HC\equiv COH$	1391.1	622.9	4.6	82.7
$HC\equiv CSH$	1386.5	705.6		

$\Delta_{acidity}$ and $\Delta_{basicity}$ are the acidity and basicity differences between OH- and SH-containing derivatives, when the CC bond order goes from one to two and from two to three, respectively. All values in $kJ\cdot mol^{-1}$

^aThe experimental acidities for CH_3-CH_2OH and CH_3-CH_2SH are 1586.2 ± 0.42 and $1488. \pm 8.8$ $kJ\cdot mol^{-1}$, respectively (see ref. [35])

^bThe experimental basicities for CH_3-CH_2OH and CH_3-CH_2SH are 776.4 and 789.6 $kJ\cdot mol^{-1}$, respectively (see ref. [35])

the experimental values, showing indeed that the gap between the acidities (99.8 $kJ\cdot mol^{-1}$) is almost one order of magnitude larger than the gap between the basicities

(15.1 $kJ\cdot mol^{-1}$). However, the values in the table also show that the gap for the acidities decreases significantly when the unsaturation of the C–C bond increases, whereas the opposite is observed for the corresponding basicities (see also Figure S2 of the Supporting Information). These results simply reflect that on going from $CH_3-CH_2O^-$ to $CH_2=CHO^-$, the conjugation between the C=C double bond and the C–O bond, being the O atom a first-row element, is much stronger than the same conjugation between the C=C and the C–S bond. The same happens on going from $CH_2=CHO^-$ to $CH\equiv CO^-$ to the point that in the latter, the C–O bond is practically a double bond, whereas the double-bond character of the C–S bond in the $CH\equiv CS^-$ is much smaller.

In a similar way, the basicity decreases necessarily when the C–C bond order increases because it implies an increase of the effective electronegativity of the CC group with respect to the X ($X=OH, SH$) attached to it. Accordingly, the electron donor ability of the X group decreases as well as its intrinsic basicity. However, the effect is smaller for the *thio* derivative, because S being a second-row element is more polarizable than O and the aforementioned electronegativity enhancement necessarily smaller.

4 Specificity of substituent effects

Since, as we have discussed in detail above, the substituent effects go in the same sense for the RCOOH and RCOOH families, it does not matter whether the active center for protonation or deprotonation is a OH or a SH group, in what follows, and for simplicity, we are going to focus our discussion on $RC\equiv COH$ derivatives to investigate the variation of both intrinsic properties when the first-row substituents are replaced by their second-row analogs. Rather unexpectedly, though the acidity and basicity trends follow the same patterns irrespective the nature of the active site (OH or SH),

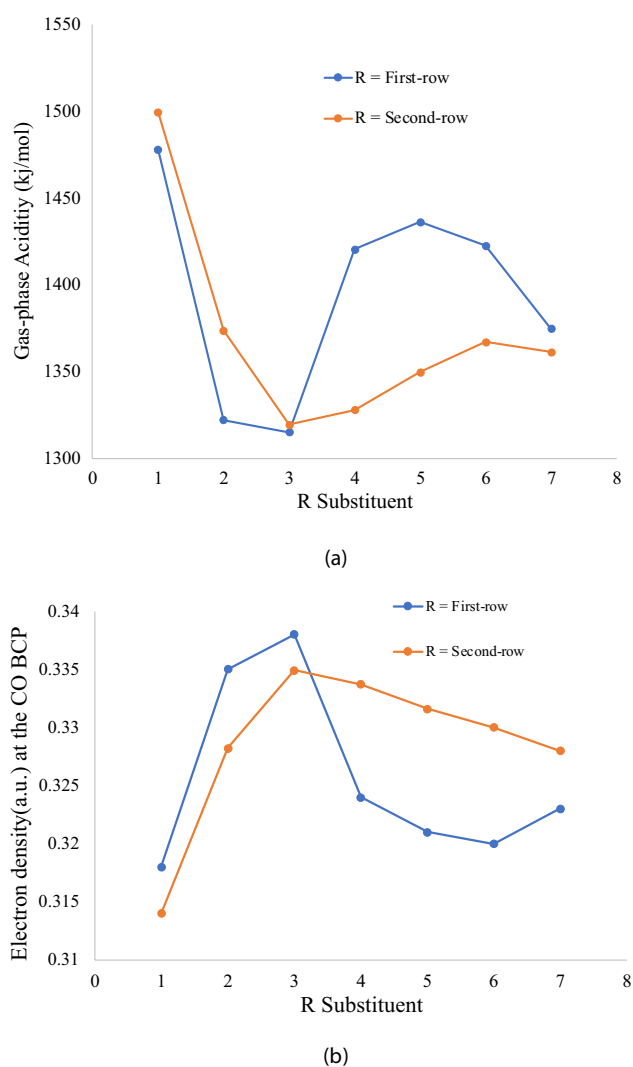


Fig. 2 Evolution of the gas-phase acidities **a** for $RC\equiv COH$ derivatives as a function of the nature of the substituent. **b** Evolution of the electron density of the C-O bond for $RC\equiv COH$ derivatives as a function of the nature of the substituent. In both figures R (1=Li, Na; 2=BeH, MgH; 3=BH₂, AlH₂; 4=CH₃, SiH₃; 5=NH₂, PH₂; 6=OH, SH and 7=F, Cl)

the trends observed when moving from the first-row substituents to second-row substituents, change significantly. Let us start our analysis with the intrinsic acidities.

As illustrated in Fig. 2a, the Li (Na) derivative is the one with the smallest acidity of the corresponding series. Going from Li to BeH and BH₂ (or from Na to MgH and AlH₂), a significant increase in the acidity of the system takes place. These trends change when the substituent is a methyl (silyl) group, with a significant decrease of its intrinsic acidity with respect to the Li, BeH and BH₂ (Na, MgH and AlH₂) derivatives, decrease that is even larger for the NH₂ substituent, for which the minimum acidity is found, with the only exception of the Li derivative. Also interestingly, the effects are qualitatively similar for the second-row substituents, but quantitatively much smaller. Another slight difference is that now the minimum acidity is observed for the SH substituent rather than for the PH₂ one.

In order to understand this peculiar behavior, we have analyzed the electron densities of the neutral, deprotonated and protonated species. In Fig. 3, we show the molecular graphs for the set of RCOOH compounds when R is a first-row substituent. For the second-row substituents, a similar information is provided in Figure S3 of the Supporting Information.

As it should be expected, the nature of the substituent has a visible effect in the electron distribution of the system and therefore in the relative strength of the bonds. The values in Fig. 3 show that the CC bond becomes systematically stronger from Li to CH₃, the effects being even slightly stronger when looking at the C-O bonds, what should have a direct effect on the acidity of the OH group. Indeed, when the electron density of the CO bond is plotted as a function of the nature of R (see Fig. 2b), it is found that its evolution is completely compatible with the variation observed for the intrinsic acidity showed in Fig. 2a. The correlations are similar when looking at the electron densities of the CO bond in the corresponding deprotonated species as shown in Figure S4 of the Supporting Information. For Li, BeH and BH₂, there is an increase in the strength of the C-O bond leading to a consistent acidity increase of the system. Also, the significant decrease of the strength of the CO bond predicted when the substituent is a methyl group is again reflected in a substantial decrease in the acidity of the system. The same consistency between the variation of the intrinsic acidities and the electron densities at the CO BCP is also observed when the substituents are second-row when Fig. 2a and b is compared, but the changes in the electron densities are attenuated with respect to those observed for the first-row substituent in a similar way as the corresponding intrinsic acidities.

The consequence is that the intrinsic acidity of the silyl derivative is almost 100 kJ·mol⁻¹ larger than that of the methyl one (see Table 1 and Fig. 2a). This very different

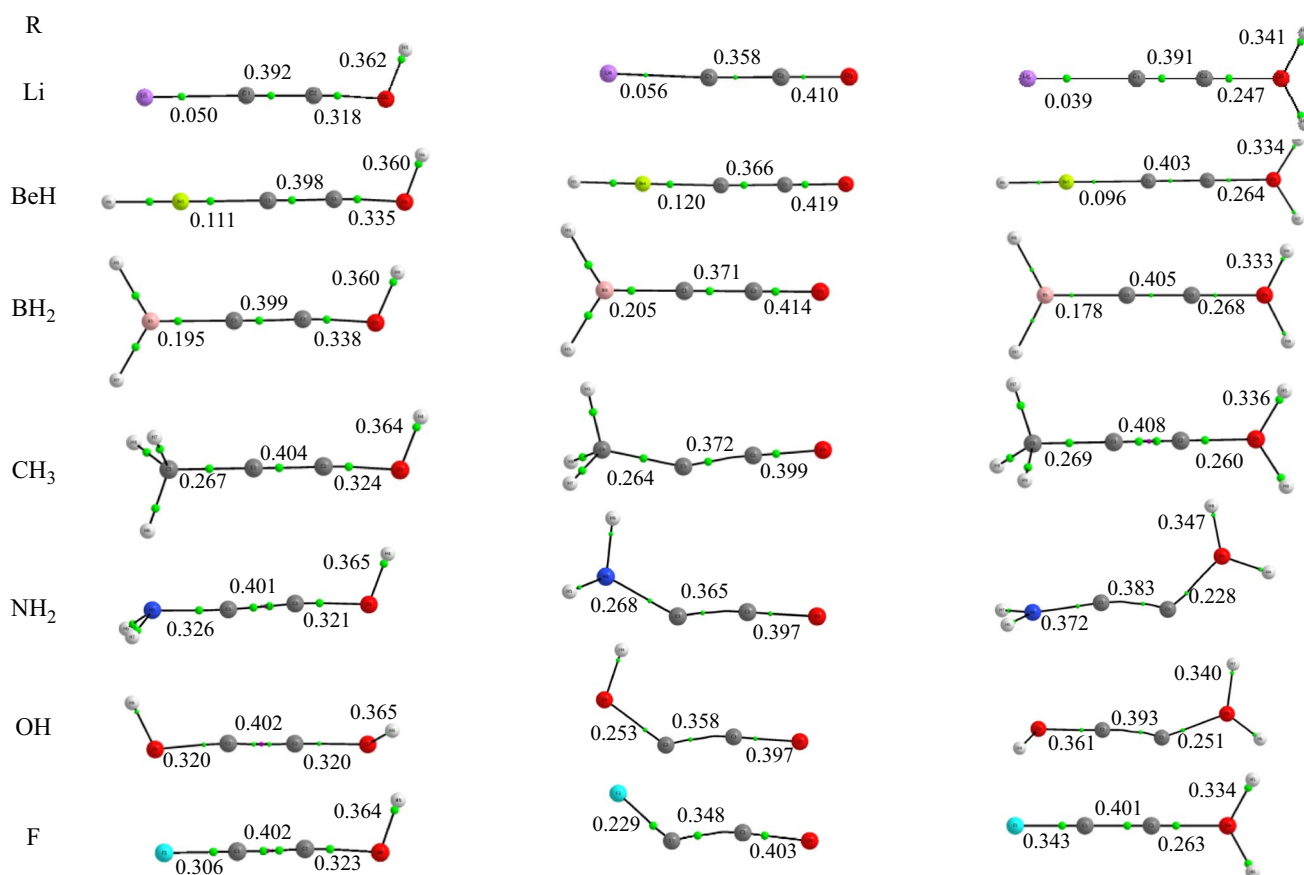


Fig. 3 Molecular graphs for the neutral, deprotonated and protonated forms of $RC\equiv COH$ derivatives. R (Li, BeH, BH_2 , CH_3 , NH_2 , OH and F). The electron densities at the BCPs are in a.u

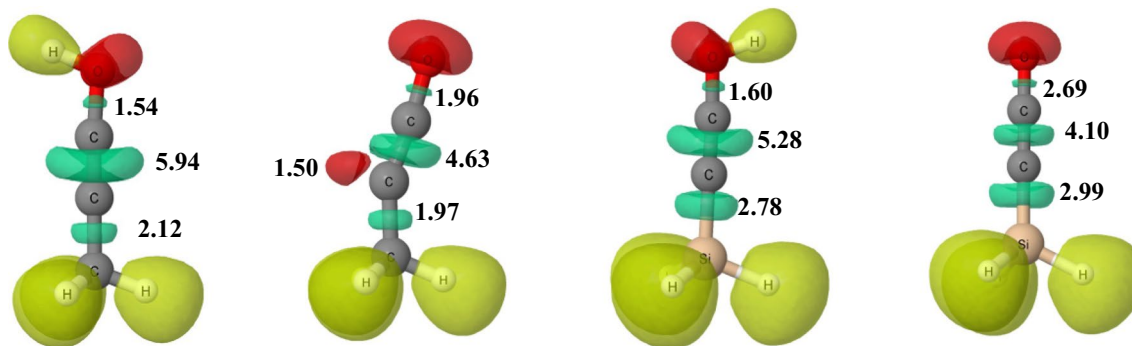


Fig. 4 ELF isosurfaces (value 0.82) of the neutral and deprotonated forms of the methyl and silyl $RC\equiv COH$ derivatives. Yellow lobes correspond to disynaptic $V(\text{atom}, H)$ basins, whereas red lobes are

monosynaptic $V(\text{atom})$ lone-pair basins and green lobes disynaptic $V(\text{atom}, \text{atom})$ basins. The electronic populations of some of the most significant disynaptic basins are indicated

behavior directly reflects the large dissimilarities observed in the bonding perturbation that the deprotonation induces in both derivatives. These differences are evident when looking at the corresponding NBO analysis and the ELF plots (see Fig. 4). The NBO calculations show that for the methyl derivative, the deprotonation of the OH bond implies

a significant electron density shift from the new lone pair at the O atom toward the CC antibonding orbital. Accordingly, the ELF analysis shows that CC disynaptic basin corresponds now to a double rather than to a triple bond, what is associated with the corresponding bending of the C–C–C group and the formation of a carbenoid basin with a

population of 1.5 e. The breaking of one of the C–C bonding interactions also results, according to the NBO analysis, in an electron density shift to the CO bonding region, so that the electron population at the C–O disynaptic basin increases from 1.54 to 1.96 e (see Fig. 4) and the C–O bond becomes 0.12 Å shorter. In the case of the silyl derivative, the deprotonation results in a significant charge delocalization along the Si–C–C–O arrangement with a significant reinforcement of both the C–O and the C–Si linkages, yielding a ketene-like electronic arrangement which maintains the linearity of the SiCCO skeleton, and is responsible of the enhanced stability of the silyl deprotonated form with respect to the methyl deprotonated one.

The direct relationship between the acidity changes and the strength of the CO bond of the compounds investigated, is ratified when the changes in the intrinsic acidities as a function of the nature of the substituents are plotted versus the dissociation energies of the CO bond of the deprotonated species evaluated at the G4 level, as shown in Fig. 5.

Fig. 5 RC≡COH compounds. Linear correlation between the acidities increases (ΔH_{acid}) when a first-row substituent (Li, BeH, BH₂, CH₃, NH₂, OH and F) is replaced by the analogous of the second row (Na, MgH, AlH₂, SiH₃, PH₂, SH and Cl) and the increase in the dissociation enthalpy of the C–O (ΔH_{CO}) bond of the anion formed upon deprotonation of the system ($\Delta H_{\text{acid}} = 0.7811 \Delta H_{\text{CO}} + 3.587$, $r^2 = 0.961$)

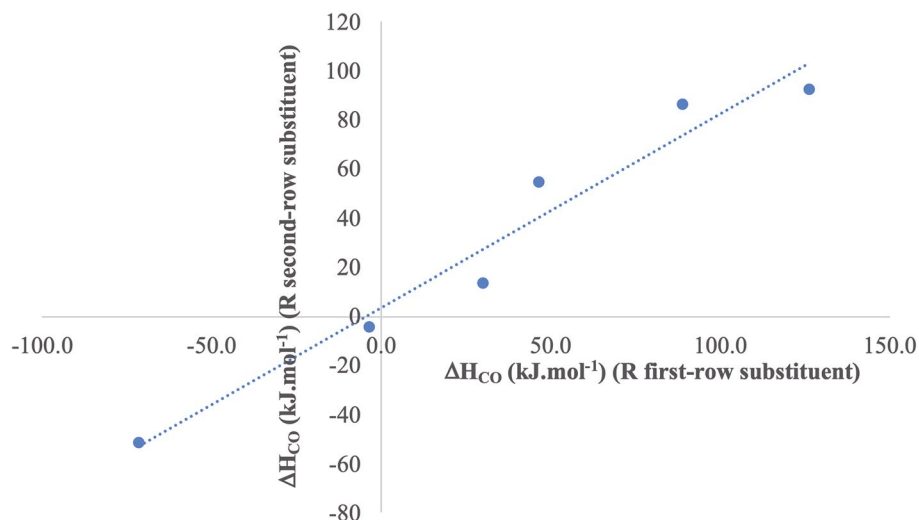
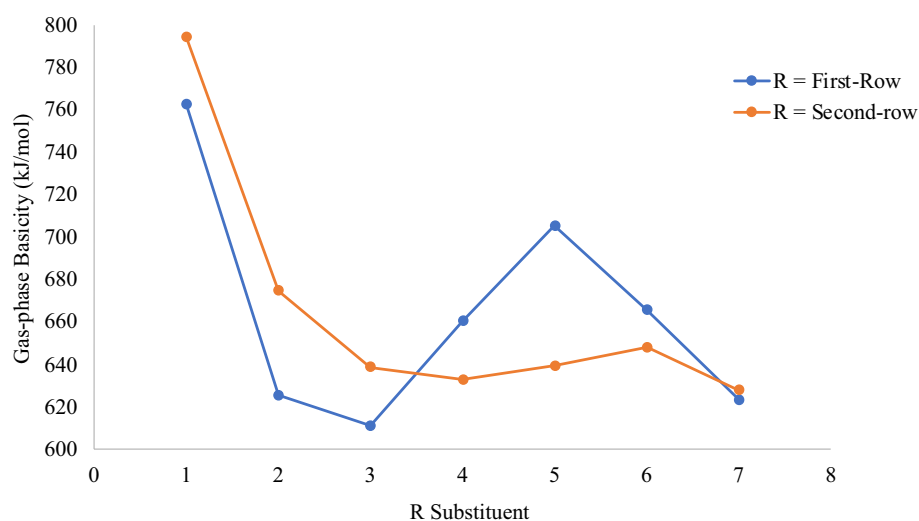


Fig. 6 Evolution of the gas-phase basicities for RC≡COH derivatives as a function of the nature of the substituent. R (1 = Li, Na; 2 = BeH, MgH; 3 = BH₂, AlH₂; 4 = CH₃, SiH₃; 5 = NH₂, PH₂; 6 = OH, SH and 7 = F, Cl)



As it could not be otherwise, the behavior observed for basicities is the opposite of that just described above for acidities. Hence, as shown in Fig. 6, on going from Li to BeH and BH₂ (or from Na to MgH and AlH₂), a significant decrease in the basicity of the system is observed, whereas a significant increase is observed for the methyl substituent, with a maximum basicity when the substituent is NH₂. These increases are again much smaller when dealing with the second-row substituents.

These trends actually reflect the changes in the strength of the new O–H bond formed upon protonation of the OH group. As it is shown in Figs. 3 and S5, on going from Li (Na) to BeH and BH₂ (MgH, AlH₂), the protonation of the OH group of the base leads to a decrease of the electron density at the corresponding OH BCPs. However, the replacement of the BH₂ group by a methyl substituent leads to an increase of this density, which reaches its maximum for the NH₂ (SH) substituent. The main consequence is again the big difference in the basicity of these compounds when one

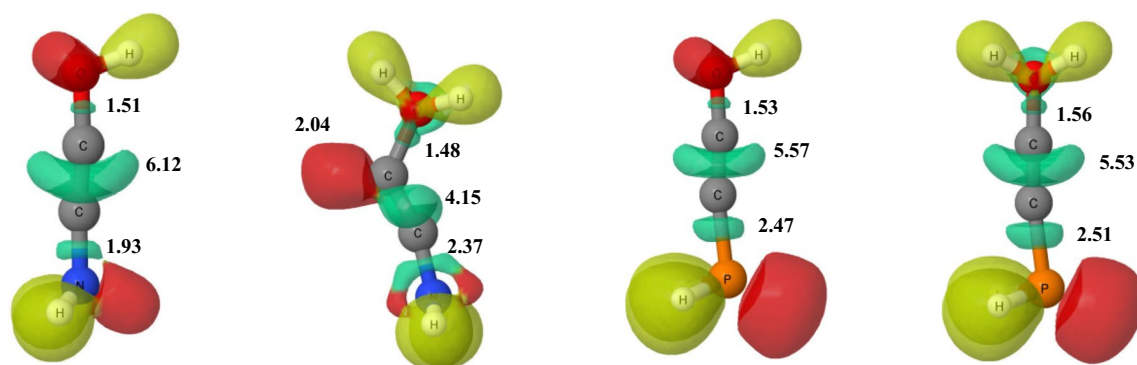


Fig. 7 ELF isosurfaces (value 0.82) of the neutral and protonated forms of the amino and phosphine $RC\equiv COH$ derivatives. Yellow lobes correspond to disynaptic $V(\text{atom}, \text{H})$ basins, whereas red lobes

compares the effect of a first-row substituent, for instance $R = \text{NH}_2$, to the effect of the second-row counterpart, $R = \text{PH}_2$, the basicity of the latter being $66 \text{ kJ}\cdot\text{mol}^{-1}$ smaller than that of the former. Again, this different behavior can be easily explained in terms of the NBO and ELF of these structures. As illustrated in Fig. 7, while no significant changes are observed in the population of the bonds of the phosphine derivative upon protonation reflecting the softer character of the PH_2 , both the NBO and ELF analyses show that the electronegativity enhancement by the OH group of the amine derivative upon protonation, strongly polarizes the electron density toward this center. Since the amino group is much less polarizable than the phosphine group, this polarization results in a depopulation the CC bonding (from 6.12 to $4.15 e^-$), which is consistent with the NBO analysis that shows that in the protonated species, the $C\equiv C$ bond is changed into a $C=C$ double bond. The high electronegativity of the amino group is also behind the substantial increase of the population at the C-N disynaptic basin, which is again consistent with the NBO analysis that indicates that the single C-N bond of the neutral is now a $C=N$ double bond in the protonated species, whereas a carbene is formed at the carbon atom bonded to the oxygen atom.

5 Concluding remarks

Our G4 calculations show that the acidity and the basicity of $R-C\equiv COH$ and $R-C\equiv CSH$ compounds follow very similar trends provided that the R substituents are the same, all are either the first-row or second-row substituents. We have also found that the gap between the acidities of the OH and SH derivatives is very small, 2% in average, whereas the basicities of the thio derivatives are found to be around 12% higher, in average, than those of the hydroxyl counterparts. This finding is in clear contrast with the experimental behavior of the $\text{CH}_3\text{-CH}_2\text{-OH}$ and $\text{CH}_3\text{-CH}_2\text{-SH}$

are monosynaptic $V(\text{atom})$ lone-pair basins and green lobes disynaptic $V(\text{atom}, \text{atom})$ basins. The electronic populations of some of the most significant disynaptic basins are indicated

saturated analogs, for which the gap between their acidities is rather large, whereas it is very small between their basicities. An exploration of the behavior of these compounds with the nature of the CC bond shows that the basicity gap increases systematically as the unsaturation of the CC bond increases; whereas, as expected for the acidity, the trend is the opposite. The most surprising finding, however, is the significant differences observed between the values of these two properties, acidity and basicity, when the first-row substituents of $R-C\equiv CX$ ($X = \text{OH}, \text{SH}$) compounds are replaced by the corresponding second-row ones. The changes found for the acidity and basicity upon changing the nature of R, reflect significant electron density redistributions leading to changes in the strength of the CC and the CX ($X = \text{OH}, \text{SH}$), in particular, for substituents whose heavy atom is at the right end of the corresponding period (C, N, O, Si, P and S); these effects being much stronger for the first-row substituents than for the second-row substituents, which are more polarizable.

Supplementary Information The online version contains supplementary material available at <https://doi.org/10.1007/s00214-023-02967-0>.

Acknowledgements This work was carried out with financial support from the projects PID2021-125207NB-C31, PID2021-125207NB-C32 and PID2019-110091GB-I00 of the Ministerio de Ciencia, Innovación y Universidades of Spain (MICINN). Finally, the authors thank the Centro de Computación Científica of the UAM (CCC-UAM) for the generous allocation of computer time and continued technical support. J.-C.G. thanks the CNES for a grant (50006558).

Author contributions M.Y., J.C.G. and I.A. wrote the main manuscript text. O.M. prepared the figures and the tables. All authors reviewed the manuscript

Funding Open Access funding provided thanks to the CRUE-CSIC agreement with Springer Nature.

Declarations

Conflicts of interest There are no conflicts to declare.

Open Access This article is licensed under a Creative Commons Attribution 4.0 International License, which permits use, sharing, adaptation, distribution and reproduction in any medium or format, as long as you give appropriate credit to the original author(s) and the source, provide a link to the Creative Commons licence, and indicate if changes were made. The images or other third party material in this article are included in the article's Creative Commons licence, unless indicated otherwise in a credit line to the material. If material is not included in the article's Creative Commons licence and your intended use is not permitted by statutory regulation or exceeds the permitted use, you will need to obtain permission directly from the copyright holder. To view a copy of this licence, visit <http://creativecommons.org/licenses/by/4.0/>.

References

- van Hemert MC, van Dishoeck EF (2008) Photodissociation of small carbonaceous molecules of astrophysical interest. *Chem Phys* 343(2–3):292–302
- Costes M, Halvick P, Hickson KM, Daugey N, Naulin C (2009) Non-threshold, threshold, and nonadiabatic behavior of the key interstellar C + C₂H₂ reaction. *Astrophys J* 703(2):1179–1187
- Largo L, Redondo P, Rayon VM, Largo A, Barrientos C (2010) The reaction between NH₃⁺ and CH₃COOH: a possible process for the formation of glycine precursors in the interstellar medium. *Astron Astrophys* 516:A79
- Simakov A, Miller GBS, Bunkan AJC, Hoffmann MR, Uggerud E (2013) The dissociation of glycolate-astrochemical and prebiotic relevance. *Phys Chem Chem Phys* 15(39):16615–16625
- Ayouz MA, Yuen CH, Balucani N, Ceccarelli C, Schneider IF, Kokoouline V (2019) Dissociative electron recombination of NH₂CHOH⁺ and implications for interstellar formamide abundance. *Mon Notices Royal Astron Soc* 490(1):1325–1331
- Xu ZX, Luo N, Federman SR, Jackson WM, Ng CY, Wang LP, Crabtree KN (2019) Ab initio study of ground-state CS photodissociation via highly excited electronic states. *Astrophys J* 882(2):86
- Richardson V, Ascenzi D, Sundelin D, Alcaraz C, Romanzin C, Thissen R, Guillemin JC, Polasek M, Tosi P, Zabka J, Gerpert WD (2021) Experimental and computational studies on the reactivity of methanimine radical cation (H₂CNH⁺) and its isomer aminomethylene (HCNH₂⁺) With C₂H₂. *Front Astron Space Sci* 8:752376
- Douglas KM, Lucas DI, Walsh C, West NA, Blitz MA, Heard DE (2022) The gas-phase reaction of NH₂ with formaldehyde (CH₂O) is not a source of formamide (NH₂CHO) in interstellar environments. *Astrophys J Lett* 937(1):L16
- Mó O, Yáñez M, Guillemin JC (2005) A theoretical study on the dimers of aminoacrylonitrile (3-amino-2-propenenitrile), a compound of astrochemical interest. *ARKIVOC* 9:239–252
- Vega-Vega A, Largo A, Redondo P, Barrientos C (2017) Structure and spectroscopic properties of Mg, C, N, O isomers: plausible astronomical molecules. *ACS Earth Space Chem* 1(3):158–167
- Redondo P, Largo A, Barrientos C (2018) Structure and spectroscopic properties of imine acetaldehyde: a possible interstellar molecule. *MNRAS* 478(3):3042–3048
- Redondo P, Largo A, Barrientos C (2020) Structure and spectroscopic properties of hydrocalcium isocyanide isomers: plausible astronomical Ca-bearing molecules. *Astrophys J* 899(2):135
- Askeland E, Mollendal H, Uggerud E, Guillemin JC, Moreno JRA, Demaison J, Huet TR (2006) Microwave spectrum, structure, and quantum chemical studies of a compound of potential astrochemical and astrobiological interest: Z-3-amino-2-propenenitrile. *J Phys Chem A* 110(46):12572–12584
- Benidar A, Georges R, Guillemin J-C, Mó O, Yáñez M (2010) Infrared spectra of a species of potential prebiotic and astrochemical interest: cyanoethenethiol (NC-CH=CH-SH). *J Phys Chem A* 114(35):9583–9588
- Benidar A, Georges R, Guillemin J-C, Mó O, Yáñez M (2013) Infrared spectra of cyanoacetaldehyde (NCCH₂CHO): a potential prebiotic compound of astrochemical interest. *Chem Phys Chem* 14(12):2764–2771
- Benidar A, Begue D, Richter F, Pouchan C, Lahcini M, Guillemin JC (2015) Gas-phase infrared spectra of three compounds of astrochemical interest: vinyl, allenyl, and propargyl isocyanides. *Chem Phys Chem* 16(4):848–854
- Shingledecker CN, Alvarez-Barcia S, Korn VH, Kastner J (2019) The case of H₂C₃O isomers, revisited: solving the mystery of the missing propadienone. *Astrophys J* 878(2):80
- Vazart F, Ceccarelli C, Balucani N, Bianchi E, Skouteris D (2020) Gas-phase formation of acetaldehyde: review and new theoretical computations. *Mon Notices Royal Astron Soc* 499(4):5547–5561
- Shingledecker CN, Molpeceres G, Rivilla VM, Majumdar L, Kastner J (2020) Isomers in interstellar environments I the case of Z- and E-cyanomethanimine. *Astrophys J* 897(2):158
- Job N, Karton A, Thirumoorthy K, Cooksy AL, Thimmakonda VS (2020) Theoretical studies of SiC₄H₂ isomers delineate three low-lying silylidenes are missing in the laboratory. *J Phys Chem A* 124(5):987–1002
- Sanz-Novo M, Leon I, Alonso JL, Largo A, Barrientos C (2020) Formation of interstellar cyanoacetamide: a rotational and computational study. *Astronomy & Astrophys* 644:A3
- Cabezas C, Agundez M, Marcelino N, Tercero B, Cuadrado S, Cernicharo J (2021) Interstellar detection of the simplest aminocarbonyl H₂NC: an ignored but abundant molecule. *Astron Astrophys* 654:A45
- Mota VC, Varandas AJC, Mendoza E, Wakelam V, Galvao BRL (2021) SiS formation in the interstellar medium through Si plus SH gas-phase reactions. *Astrophys J* 920(1):37
- Canelo CM, Bronfman L, Mendoza E, Duronea N, Merello M, Carvajal M, Friaca ACS, Lepine J (2021) Isocyanic acid (HNCO) in the hot molecular core G331.512–0.103: observations and chemical modelling. *Mon Notices Royal Astron Soc* 504(3):4428–4444
- Field-Theodore TE, Taylor PR (2022) Interstellar hide and go seek: C₃H₄ there and back (again). *Phys Chem Chem Phys* 24(32):19184–19198
- Esposito VJ, Friskey JM, Trabelsi T, Francisco JS (2022) Astrochemical significance and spectroscopy of tetratomic H, P, S, O. *Astronomy & Astrophysics* 659:A54
- Ferrero S, Zamirri L, Ceccarelli C, Witzel A, Rimola A, Ugliengo P (2020) Binding energies of interstellar molecules on crystalline and amorphous models of water ice by Ab initio calculations. *Astrophys J* 904(1):11
- Bovolenta G, Bovino S, Vohringer-Martinez E, Saez DA, Grassi T, Vogt-Geisse S (2020) High level ab initio binding energy distribution of molecules on interstellar ices: hydrogen fluoride. *Mol Astrophys* 21:100095
- Perrero, J.; Rimola, A.; Corno, M.; Ugliengo, P. In Ab initio calculation of binding energies of interstellar sulphur-containing species on crystalline water ice models, In: 21st international conference on computational science and its applications (ICCSA), Cagliari, ITALY, Sep 13–16; Cagliari, ITALY, 2021; pp 608–619.
- Simmie JM, Wurmel J (2020) An organized collection of theoretical gas-phase geometric, spectroscopic, and thermochemical data of oxygenated hydrocarbons, C_xH_yO_z (x, y=1, 2; z=1–8), of relevance to atmospheric, astrochemical, and combustion sciences. *J Phys Chem Ref Data* 49(2):023102

31. Rivilla VM, Colzi L, Jimenez-Serra I, Martin-Pintado J, Megias A, Melosso M, Bizzocchi L, Lopez-Gallifa A, Martinez-Henares A, Massalkhi S, Tercero B, de Vicente P, Guillemin JC, de la Concepcion JG, Rico-Villas F, Zeng SS, Martin S, Requena-Torres MA, Tonolo F, Alessandrini S, Dore L, Barone V, Puzzarini C (2022) Precursors of the RNA world in space: detection of (Z)-1,2-ethenediol in the interstellar medium, a key intermediate in sugar formation. *Astrophys J Lett* 929(1):L11
32. Turecek F, Havlas Z (1986) Thermochemistry of unstable enols - the O-(CD)(H) group equivalent. *J Org Chem* 51(21):4066–4067
33. Hart H (1979) Simple Enols. *Chem Rev* 79(6):515–528
34. Belloche A, Menten KM, Comito C, Mueller HSP, Schilke P, Ott J, Thorwirth S, Hieret C (2008) Detection of amino acetonitrile in Sgr B2(N) (vol482, pg 179, 2008). *Astron Astrophys* 492(3):769–773
35. Curtiss LA, Redfern PC, Raghavachari K (2007) Gaussian-4 theory. *J Chem Phys* 126(8):084108
36. Hunter EP, Lias SG (1998) Evaluated gas phase basicities and proton affinities of molecules: an update. *J Phys Chem Ref Data* 27:413–656
37. DeTuri VF, Ervin KM (1999) Competitive threshold collision-induced dissociation: gas-phase acidities and bond dissociation energies for a series of alcohols. *J Phys Chem A* 103:6911–6920
38. Janousek BK, Reed KJ, Brauman JI (1980) Electron photodetachment from mercaptyl anions (RS⁻ electron affinities of mercaptyl radicals and the S-H bond strength in mercaptans). *J Am Chem Soc* 102:3125–3129
39. Bader RFW (1990) *Atoms in molecules A Quantum Theory*. Clarendon Press, Oxford
40. Reed AE, Weinhold F (1985) Natural localized molecular-orbitals. *J Chem Phys* 83(4):1736–1740
41. Savin A, Nesper R, Wengert S, Fassler TF (1997) ELF: the electron localization function. *Angew Chem-Int Edit* 36(17):1809–1832
42. Keith TA. AIMAll (Version 19.10.12), TK Gristmill Software: Overland Parks KS, 2019; <https://aim.tkgristmill.com>
43. Smith BJ, Radom L, Kresge AJ (1989) Ethynol: a theoretical prediction of remarkably high gas-phase acidity. *J Am Chem Soc* 111:8297–8299
44. Guillemin JC, Riague EH, Gal JF, Maria PC, Mó O, Yáñez M (2005) Acidity trends in alpha, beta-unsaturated sulfur, selenium, and tellurium derivatives: comparison with C-, Si-, Ge-, Sn-, N-, P-, As-, and Sb-containing analogues. *Chem-Eur J* 11(7):2145–2153
45. Martin JDD, Hepburn JW (1998) Determination of bond dissociation energies by threshold ion-pair production spectroscopy: An improved D-0(HCl). *J Chem Phys* 109:8139–8142
46. Chiang Y, Kresge AJ, Hochstrasser R, Wirz J (1989) Phenyl- and mesitylnol. The first generation and direct observation of hydroxyacetylenes in solution. *J Am Chem Soc* 111:2355–2357

Publisher's Note Springer Nature remains neutral with regard to jurisdictional claims in published maps and institutional affiliations.